IET Renewable Power Generation

Special Issue Call for Papers

Be Seen. Be Cited.
Submit your work to a new IET special issue

Connect with researchers and experts in your field and share knowledge.

Be part of the latest research trends, faster.

Read more

The Institution of Engineering and Technology

IET Renewable Power Generation

Research Article

IET Journals
The Institution of Engineering and Technology

Power management of an isolated hybrid AC/DC micro-grid with fuzzy control of battery banks

ISSN 1752-1416
Received on 21st August 2014
Accepted on 13th November 2014
doi: 10.1049/iet-rpg.2014.0271
www.ietdl.org

Mehdi Hosseinzadeh ✉, *Farzad Rajaei Salmasi* ✉

School of Electrical and Computer Engineering, College of Engineering, University of Tehran, PO Box 14395/515, Tehran, Iran
✉ *E-mail: mehdi.hosseinzadeh@ieee.org, farzad–rs@ieee.org*

Abstract: This study focuses on the development of a supervisory control scheme for power management and operation of an isolated hybrid AC/DC micro-grid, which consists of an AC micro-grid and a DC micro-grid. In the proposed hybrid micro-grid, wind and diesel generators and AC loads are connected to the AC micro-grid, whereas photovoltaic array and DC loads are tied to the DC micro-grid. Moreover, the authors consider two independent battery banks in the AC and DC micro-grids. Furthermore, the AC and the DC micro-grids are coupled through a bidirectional converter, which can act as an inverter or rectifier. The objectives of the proposed supervisory controller are listed as follows: (i) maximum utilisation of renewable energy sources along with satisfying the load power demand in both AC and DC micro-grids, (ii) maintaining state of charge (SOC) of battery banks in both AC and DC micro-grids and (iii) managing the power exchange between the AC and the DC micro-grids while the reliability of the whole system is taken into account. The supervisory controller is formalised using a state machine approach. For these purposes, 15 distinct operation modes are considered. Furthermore, in order to extend the battery life cycle, a fuzzy controller manages the desired SOC controlling the charge and discharge currents. The effectiveness of the proposed supervisory controller is evaluated through extensive numerical simulations.

Nomenclature

DG	diesel generator
PMSG	permanent magnetic synchronous generator
PV	photovoltaic
SOC	state of charge
WG	wind generator
A	turbine swept area
B	cell deviation from the ideal p–n junction characteristic
C, L	electrical parameters of the DC/DC converter in PV
$C_{\mathrm{b}}^{\mathrm{AC}}$, $C_{\mathrm{b}}^{\mathrm{DC}}$	capacitance in the model of battery bank in AC and DC micro-grids, respectively
C_{p}, C_{t}	performance and torque coefficients, respectively
$E_{\mathrm{b}}^{\mathrm{AC}}$, $E_{\mathrm{b}}^{\mathrm{DC}}$	voltage source in the model of battery bank in AC and DC micro-grids, respectively
E_{G}	bandgap energy of the semiconductor used in the cell
i_d^{DG}, i_q^{DG}	terminal currents in the d–q axes for DG
i_d^{WG}, i_q^{WG}	terminal currents in the d–q axes for WG
I_{diesel}	fuel injection system input signal
i_L^{AC}, i_L^{AC}	corresponds to the power demand in AC and DC micro-grids, respectively
$i_{\mathrm{m}}^{\mathrm{AC}}$, $i_{\mathrm{m}}^{\mathrm{AC}}$	corresponds to the power injected from AC to DC micro-grids, and vice versa, respectively
$i_{\mathrm{o}}^{\mathrm{WG}}$, $i_{\mathrm{o}}^{\mathrm{DG}}$, $i_{\mathrm{o}}^{\mathrm{PV}}$	output current of WG, DG and PV, respectively
I_{ph}	generated current under a given isolation
i_{PV}, v_{PV}	current and voltage of PV
I_{rr}, I_{rs}	reverse saturation current, and reverse saturation current at T_{r}, respectively
I_{scr}	cell short-circuit current
J_{WG}, J_{DG}	inertia of the rotating system in WG and DG
K	Boltzmann's constant
K_i	short-circuit current temperature coefficient
k_{tr}, δ	winding ratio of the transformer included in the DC/DC converter and its duty cycle, respectively
L_d^{DG}, L_q^{DG}	stator inductances in the d–q axes for DG
L_d^{WG}, L_q^{WG}	stator inductances in the d–q axes for WG
M_{WG}, M_{DG}	number of poles in WG and DG
ns_{p}, n_{s}	number of parallel and series modules
P_{WG}, P_{DG}, P_{PV}	output power of WG, DG and PV, respectively
P_{AC2DC}, P_{DC2AC}	power injected from AC to DC micro-grids, and vice versa, respectively
$P_{\mathrm{Batt}}^{\mathrm{AC}}$, $P_{\mathrm{Batt}}^{\mathrm{DC}}$	output power of the battery bank in AC and DC micro-grids, respectively
$P_{\mathrm{critical}}^{\mathrm{WG}}$, $P_{\mathrm{critical}}^{\mathrm{PV}}$	critical power for WG and PV, respectively
$P_{\mathrm{gen}}^{\mathrm{AC}}$, $P_{\mathrm{gen}}^{\mathrm{DC}}$	total generated power in AC and DC micro-grids, respectively
P_L^{AC}, P_L^{DC}	power demand in AC and DC micro-grids, respectively
$p_{\mathrm{m}}^{\mathrm{WG}}$, $p_{\mathrm{m}}^{\mathrm{DG}}$	turbine mechanical output power in WG and DG, respectively
$p_{\mathrm{max}}^{\mathrm{WG}}$, $p_{\mathrm{max}}^{\mathrm{DG}}$, $p_{\mathrm{max}}^{\mathrm{PV}}$	maximum power of WG, DG and PV, respectively
$p_{\mathrm{ref}}^{\mathrm{WG}}$, $p_{\mathrm{ref}}^{\mathrm{DG}}$, $p_{\mathrm{ref}}^{\mathrm{PV}}$	reference power of WG, DG and PV, respectively
q	charge of an electron
$Q_{\mathrm{c,AC}}^{\mathrm{max}}$, $Q_{\mathrm{c,DC}}^{\mathrm{max}}$	maximum capacity of the battery bank in AC and DC micro-grids, respectively
$R_{\mathrm{b}}^{\mathrm{AC}}$, $R_{\mathrm{b}}^{\mathrm{DC}}$	resistance in the model of battery bank in AC and DC micro-grids, respectively
$R_{\mathrm{s}}^{\mathrm{WG}}$, $R_{\mathrm{s}}^{\mathrm{DG}}$	synchronous resistance, of WG and DG, respectively
$\mathrm{SOC}_{\mathrm{AC}}$, $\mathrm{SOC}_{\mathrm{DC}}$	SOC of battery bank in AC and DC micro-grids, respectively
$\mathrm{SOC}_{\mathrm{AC}}^{\mathrm{dec}}$, $\mathrm{SOC}_{\mathrm{DC}}^{\mathrm{dec}}$	desired SOC of battery bank in AC and DC micro-grids, respectively

T	cell temperature
t_d	dead time of the diesel engine
T_r	cell reference temperature
T_t^{WG}, T_t^{DG}	turbine torque in WG and DG, respectively
u_{WG}, u_{DG}, u_{PV}	control signal for WG, DG and PV, respectively
v_b^{AC}, v_b^{DC}	voltage of bus O_{DC} in the AC micro-grid, and DC bus in the DC micro-grid, respectively
v_b^{AC}, v_b^{DC}	voltage of capacitance in the model of battery bank in AC and DC micro-grids, respectively
v_d^{DG}, v_q^{DG}	terminal voltages in the d–q axes for DG
v_d^{WG}, v_q^{WG}	terminal voltages in the d–q axes for WG
v_{max}^{PV}, i_{max}^{PV}	voltage and current corresponding to maximum PV output power
v_{wind}	wind speed
λ	solar radiation
ΔPWG, ΔP_{PV}	unexploited power of wind and solar subsystem, respectively
λ	tip-speed ratio of wind turbine
ρ	air density
σ, ξ_{max}	design constants
τ_{pm}, k_{pm}	fuel injection system parameters
ϕ_m^{WG}, ϕ_m^{DG}	flux linked by the stator windings in WG and DG, respectively
ω_e^{WG}, ω_e^{DG}	electrical angular speed in WG and DG, respectively
ω_m	angular shaft speed in WG
NB	negative big
NS	negative small
PB	positive big
PS	positive small
ZO	zero

1 Introduction

The rising rate of consumption of nuclear and fossil fuels, and the need of reducing pollutant emission in the electricity generation field, are the most significant reasons for worldwide attention to the renewable energy resources. In this context, micro-grids are defined as a cluster of loads, distributed energy sources and storage devices [1–6]. It is accepted that for excellent operation of the micro-grid, a supervisory controller to manage the power split between different energy sources is essential, which is called power management system. A widely used scheme for power management systems is rule-based approach, which is simple and robust, and manages the system according to some prefixed rules, as indicated in [7, 8]. In recent years, several attempts have been made to design a rule-based supervisory control system for micro-grids [9–16]. In [9], a supervisory control framework is designed for a stand-alone wind-solar system, constructing a DC micro-grid, which determines the operating mode, and manages the power according to the determined mode. Its most attractive feature is that decision algorithm of the supervisor controller is based on some measurable system variables. In [10], an isolated DC micro-grid, including wind, solar and fuel cell as energy sources is proposed. Assuming that the main generation role is the responsibility of the wind subsystem, while the solar subsystem plays a complementary role, and also depending on the load requirements, state-of charge of the battery and available power by solar and wind subsystems, five different operating modes are defined. In [11], an isolated AC micro-grid including photovoltaic (PV) array and micro-gas turbine as energy sources, and battery and ultra-capacitor as storage devices, is presented. In this paper, a central energy management system is designed, which manages the system according to the electrical output power of PV array and ultra-capacitor voltage. It should be remarked that three distinct operating modes are considered in this paper. In [12], a controller is developed to charge/discharge battery bank such that solar/wind farm power output can be dispatched. Although the proposed micro-grid is connected to the utility grid, no load is connected to the micro-grid and it can only inject power to the grid. The proposed rules are based on state-of-charge and battery current limitations. In [13], an AC-linked hybrid wind/PV/fuel cell alternative energy system for stand-alone applications is presented, in which two different operating modes are considered. A DC micro-grid consisting of a fuel cell and battery is presented in [14]. A supervisory controller is used to manage the operating modes of the system, which selects the proper mode among three possible operating modes. Corresponding to each operating mode, there is a fuzzy-based controller which determines the output of the fuel cell. Another attempt in the case of fuel cell/battery DC micro-grid is presented in [15]. In this paper, and based on the battery voltage, three operating modes are defined to determine the output current of the fuel cell. In [16], a fuzzy-based supervisory controller with five predefined rules is proposed for a DC fuel cell/battery micro-grid. It is worth noting that the rules are based on state-of-charge of the battery and the power demanded by sources.

All the above mentioned works have focused on a DC or AC micro-grid. A hybrid AC/DC micro-grid is a new concept, which couples DC sources with DC loads and AC sources with AC loads [17, 18]. A typical hybrid AC/DC micro-grid configuration, which is also used in this paper, is shown in Fig 1, where PV panel, wind turbine and diesel generator (DG) are used as power generation sources. Here, we consider an isolated hybrid micro-grid. For hybrid AC/DC micro-grids, a power management system is proposed based on the power balance equation and state-of-charge of the battery in [19], where five different operating modes are presented, such that each individual component of the micro-grid operate based on the selected mode.

In this paper, a rule-based power management system for an isolated hybrid AC/DC micro-grid is developed, where 15 distinct operation modes are defined, which is further divided into 17 states that are expressed using a state machine approach. Also, because of the intermittent nature of the wind and the solar energy, a DG is used as a back-up source to increase the reliability of the system. It is noteworthy that the operation modes are defined in a manner that minimises the operation of the DG. Furthermore, for the sake of high reliability and power quality, utilisation of the power converters between the AC and DC micro-grids are reduced. Moreover, two separate battery banks for AC and DC micro-grids are considered, where in order to achieve the desired state of charge (SOC) of battery banks, a fuzzy controller is designed to control the charge and discharge currents.

The remainder of this paper is organised as follows. Section 2 gives a brief overview of the renewable power source models and their corresponding converters, where the models of wind turbine and DG as power sources of the AC micro-grid are given in Section 2.1, and a model of PV panel as a source of the DC micro-grid is given in Section 2.2. In Section 3, a supervisor controller to coordinating between the AC and DC micro-grids is proposed, in which different operating modes are programmed in order to manage the power split between the AC and DC micro-grids. Simulation results obtained with the proposed supervisory controller are reported in Section 4. Finally, conclusion section summarises the main outcome of this paper.

2 System modelling

2.1 AC micro-grid modelling

Topology of the AC micro-grid under consideration in this paper is depicted in Fig. 1, which is based on a DG and a wind generator (WG) working in parallel. The WG system includes a windmill, multipolar permanent magnet synchronous generator (PMSG), rectifier and DC/DC converter. It should be noted that the power generated by the wind turbine is controlled through the corresponding DC/DC converter.

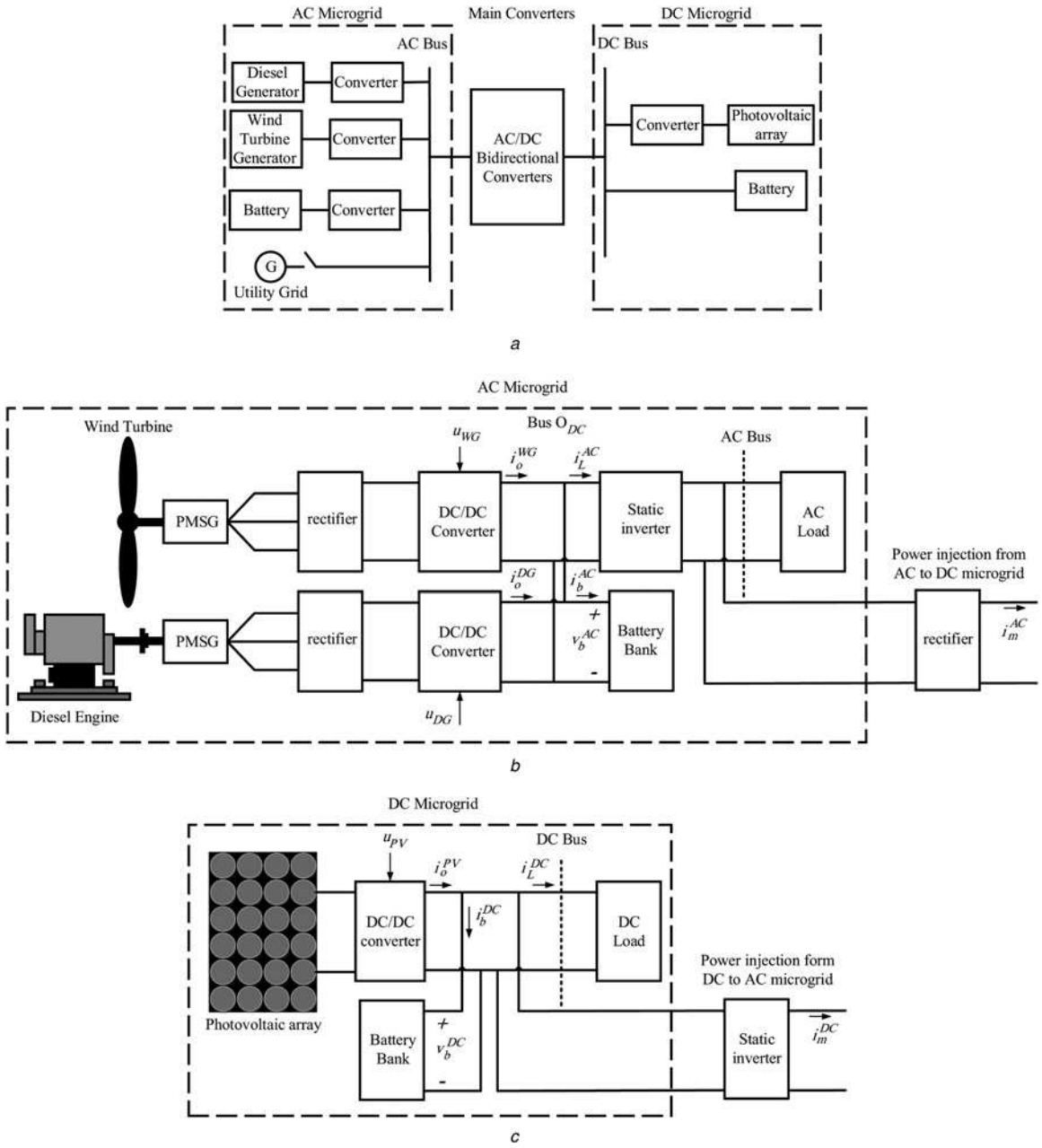

Fig. 1 *Hybrid AC/DC micro-grid*

a Typical hybrid AC/DC micro-grid configuration
b AC micro-grid schemes
c DC micro-grid schemes

The turbine mechanical output power expressed in W can be calculated by the following equation

$$p_{\mathrm{m}}^{\mathrm{WG}} = \frac{1}{2} C_{\mathrm{p}}(\lambda) \rho A v_{\mathrm{wind}}^{3} \tag{1}$$

It is worth noting that $C_{\mathrm{p}}(\lambda)$ is performance coefficient of the turbine and is modelled as follows [20]

$$C_{\mathrm{p}}(\lambda) = C_1 \left(\frac{C_2}{\lambda_i} - C_3 \right) e^{-C_4/\lambda_i} + C_5 \lambda \tag{2}$$

where

$$\frac{1}{\lambda_i} = \frac{1}{\lambda} - 0.035, \quad C_1 = 0.5176, \quad C_2 = 116, \quad C_3 = 5, \quad C_4 = 21, \quad C_5 = 0.0068$$

Furthermore, the wind turbine torque is given by

$$T_{\mathrm{t}}^{\mathrm{WG}} = \frac{p_{\mathrm{m}}^{\mathrm{WG}}}{\omega_m} = \frac{1}{2} C_{\mathrm{t}}(\lambda) \rho A r v_{\mathrm{wind}}^{2} \tag{3}$$

where $C_{\mathrm{t}}(\lambda) = C_{\mathrm{p}}(\lambda)/\lambda$ is torque coefficient of the turbine.

As shown in Fig. 1, the wind turbine is linked with a PMSG, whose dynamic model in a rotor reference frame is given by the following equations [21

$$\begin{cases} i_q^{\mathrm{WG}} = -\dfrac{R_{\mathrm{s}}^{\mathrm{WG}}}{L_q^{\mathrm{WG}}} i_q^{\mathrm{WG}} - \omega_{\mathrm{e}}^{\mathrm{WG}} i_d^{\mathrm{WG}} + \dfrac{\omega_{\mathrm{e}}^{\mathrm{WG}} \phi_{\mathrm{m}}^{\mathrm{WG}}}{L_q^{\mathrm{WG}}} - \dfrac{v_q^{\mathrm{WG}}}{L_q^{\mathrm{WG}}} \\ i_d^{\mathrm{WG}} = -\dfrac{R_{\mathrm{s}}^{\mathrm{WG}}}{L_d^{\mathrm{WG}}} i_d^{WG} - \omega_{\mathrm{e}}^{\mathrm{WG}} i_q^{\mathrm{WG}} - \dfrac{v_d^{\mathrm{WG}}}{L_d^{\mathrm{WG}}} \end{cases} \tag{4}$$

IET Renew. Power Gener., 2015, Vol. 9, Iss. 5, pp. 484–493

It is worth noting that in actual radial flux PMSGs with a smooth air-gap, it holds $L_q^{\mathrm{WG}} \cong L_d^{\mathrm{WG}} = L_{\mathrm{WG}}$. The terminal voltages (v_d^{WG}, v_q^{WG}) can also be written as

$$v_d^{\mathrm{WG}} = \frac{\pi v_b^{\mathrm{AC}} i_d^{\mathrm{WG}}}{3\sqrt{3}\sqrt{(i_d^{\mathrm{WG}})^2 + (i_q^{\mathrm{WG}})^2}} u_{\mathrm{WG}}$$
$$v_q^{\mathrm{WG}} = \frac{\pi v_b^{\mathrm{AC}} i_q^{\mathrm{WG}}}{3\sqrt{3}\sqrt{(i_d^{\mathrm{WG}})^2 + (i_q^{\mathrm{WG}})^2}} u_{\mathrm{WG}} \tag{5}$$

where $u_{\mathrm{WG}} = k_{\mathrm{tr}}/\delta$ in which k_{tr} is the winding ratio of the transformer included in the DC/DC converter and δ is the DC/DC converter duty cycle. Thus, (4) can be rewritten as (see (6))

The electrical load torque produced by the PMSG can also be calculated as

$$T_{\mathrm{e}}^{\mathrm{WG}} = \frac{3}{2}\frac{M_{\mathrm{WG}}}{2}\phi_{\mathrm{m}}^{\mathrm{WG}} i_q^{\mathrm{WG}} \tag{7}$$

Besides, assuming an ideal static conversion, the output current of the DC/DC converter is

$$i_{\mathrm{o}}^{\mathrm{WG}} = \frac{\pi}{2\sqrt{3}}\sqrt{(i_d^{\mathrm{WG}})^2 + (i_q^{\mathrm{WG}})^2} u_{\mathrm{WG}} \tag{8}$$

The diesel generation system is also constituted by a diesel prime mover, multipolar PMSG, rectifier and DC/DC converter, such that the power generated by the DG is controlled through the corresponding DC/DC converter. Here, the modelling of electrical part is neglected because of the similarity. The transfer function of the model of prime mover is as follows [22]

$$\frac{p_{\mathrm{m}}^{\mathrm{DG}}}{I_{\mathrm{diesel}}} = \frac{k_{\mathrm{pm}}}{\tau_{\mathrm{pm}} s + 1} e^{-t_{\mathrm{d}} s} \tag{9}$$

where t_{d} is the dead time of the diesel engine, which is composed of the time elapsed until the actuator actually injects fuel into the cylinder, fuel burning time to produce torque and duration until all cylinders produce torque.

The bus O_{DC} delivers the energy generated by the WG and DG to the AC load, and if necessary, to the battery bank, which is used as an energy storage system [23]. Also, its voltage is imposed by the battery bank. Here, a lead-acid battery bank is modelled as a voltage source $E_{\mathrm{b}}^{\mathrm{AC}}$ connected in series with a resistance $R_{\mathrm{b}}^{\mathrm{AC}}$ and a capacitance $C_{\mathrm{b}}^{\mathrm{AC}}$. Thus, the bus O_{DC} voltage ($v_{\mathrm{b}}^{\mathrm{AC}}$) can be written as

$$v_{\mathrm{b}}^{\mathrm{AC}} = E_{\mathrm{b}}^{\mathrm{AC}} + v_{\mathrm{c}}^{\mathrm{AC}} + \left(\frac{\pi}{2\sqrt{3}}\sqrt{(i_d^{\mathrm{WG}})^2 + (i_q^{\mathrm{WG}})^2} u_{\mathrm{WG}} + \frac{\pi}{2\sqrt{3}}\sqrt{(i_d^{\mathrm{DG}})^2 + (i_q^{\mathrm{DG}})^2} u_{\mathrm{DG}} - i_L^{\mathrm{AC}}\right) R_{\mathrm{b}}^{\mathrm{AC}} \tag{10}$$

Also, assuming an ideal inverter, the AC load current can be referred to the bus O_{DC} as an output variable current i_L^{AC}.

Finally, whole dynamic model of the AC micro-grid will be as follows (see (11))

It should be noted that $i_{\mathrm{m}}^{\mathrm{AC}}$, shown in Fig 1 corresponds to the power injected from the AC micro-grid to the DC micro-grid.

2.2 DC micro-grid modelling

The DC micro-grid, as shown in Fig. 1, comprises a PV array connected to the DC bus through a DC/DC converter, which controls operation point of the array. Generated current by PV array is calculated based on the following equation [24]

$$i_{\mathrm{PV}} = n_{\mathrm{p}} I_{\mathrm{ph}} - n_{\mathrm{p}} I_{\mathrm{rs}} \left(e^{q v_{\mathrm{PV}}/n_{\mathrm{s}} \mathrm{BKT}} - 1\right) \tag{12}$$

Also, I_{ph} and I_{rs} are determined as follows

$$I_{\mathrm{ph}} = [I_{\mathrm{scr}} + K_i (T - T_{\mathrm{r}})]\frac{\gamma}{100}$$
$$I_{\mathrm{rs}} = I_{\mathrm{rr}}\left[\frac{T}{T_{\mathrm{r}}}\right]^3 e^{q E_{\mathrm{G}}/\mathrm{KT}[1/T_{\mathrm{r}} - 1/T]} \tag{13}$$

Similar to the AC micro-grid, DC bus delivers the energy generated

$$\begin{cases} i_q^{\mathrm{WG}} = -\dfrac{R_{\mathrm{s}}^{\mathrm{WG}}}{L_{\mathrm{WG}}} i_q^{\mathrm{WG}} - \omega_{\mathrm{e}}^{\mathrm{WG}} i_d^{\mathrm{WG}} + \dfrac{\omega_{\mathrm{e}}^{\mathrm{WG}} \phi_{\mathrm{m}}^{\mathrm{WG}}}{L_{\mathrm{WG}}} - \dfrac{\pi v_{\mathrm{b}}^{\mathrm{AC}} i_q^{\mathrm{WG}}}{3\sqrt{3} L_{\mathrm{WG}} \sqrt{(i_d^{\mathrm{WG}})^2 + (i_q^{\mathrm{WG}})^2}} u_{\mathrm{WG}} \\ i_d^{\mathrm{WG}} = -\dfrac{R_{\mathrm{s}}^{\mathrm{WG}}}{L_{\mathrm{WG}}} i_d^{\mathrm{WG}} - \omega_{\mathrm{e}}^{\mathrm{WG}} i_q^{\mathrm{WG}} - \dfrac{\pi v_{\mathrm{b}}^{\mathrm{AC}} i_d^{\mathrm{WG}}}{3\sqrt{3} L_{\mathrm{WG}} \sqrt{(i_d^{\mathrm{WG}})^2 + (i_q^{\mathrm{WG}})^2}} u_{\mathrm{WG}} \end{cases} \tag{6}$$

$$\begin{cases} i_q^{\mathrm{WG}} = \dfrac{R_{\mathrm{s}}^{\mathrm{WG}} L_{\mathrm{WG}}}{i_q^{\mathrm{WG}}} - \omega_{\mathrm{e}}^{\mathrm{WG}} i_d^{\mathrm{WG}} + \dfrac{\omega_{\mathrm{e}}^{\mathrm{WG}} \phi_{\mathrm{m}}^{\mathrm{WG}}}{L_{\mathrm{WG}}} - \dfrac{\pi v_{\mathrm{b}}^{\mathrm{AC}} i_q^{\mathrm{WG}}}{3\sqrt{3} L_{\mathrm{WG}} \sqrt{(i_d^{\mathrm{WG}})^2 + (i_q^{\mathrm{WG}})^2}} u_{\mathrm{WG}} \\ i_d^{\mathrm{WG}} = -\dfrac{R_{\mathrm{s}}^{\mathrm{WG}}}{L_{\mathrm{WG}}} i_d^{\mathrm{WG}} - \omega_{\mathrm{e}}^{\mathrm{WG}} i_q^{\mathrm{WG}} - \dfrac{\pi v_{\mathrm{b}}^{\mathrm{AC}} i_d^{\mathrm{WG}}}{3\sqrt{3} L_{\mathrm{WG}} \sqrt{(i_d^{\mathrm{WG}})^2 + (i_q^{\mathrm{WG}})^2}} u_{\mathrm{WG}} \\ \dot{\omega}_{\mathrm{e}}^{\mathrm{WG}} = \dfrac{M_{\mathrm{WG}}}{2J_{\mathrm{WG}}}\left(T_{\mathrm{t}}^{\mathrm{WG}} - \dfrac{3}{2}\dfrac{M_{\mathrm{WG}}}{2}\phi_{\mathrm{m}}^{\mathrm{WG}} i_q^{\mathrm{WG}}\right) \\ i_q^{\mathrm{DG}} = \dfrac{R_{\mathrm{s}}^{\mathrm{DG}} L_{\mathrm{DG}}}{i} i_d^{\mathrm{DG}} - \omega_{\mathrm{e}}^{\mathrm{DG}} i_{\mathrm{d}}^{\mathrm{DG}} + \dfrac{\omega_{\mathrm{e}}^{\mathrm{DG}} \phi_{\mathrm{m}}^{\mathrm{DG}}}{L_{DG}} - \dfrac{\pi v_{\mathrm{b}}^{\mathrm{AC}} i_q^{\mathrm{DG}}}{3\sqrt{3} L_{\mathrm{DG}} \sqrt{(i_d^{\mathrm{DG}})^2 + (i_q^{\mathrm{DG}})^2}} u_{\mathrm{DG}} \\ i_d^{\mathrm{DG}} = -\dfrac{R_{\mathrm{s}}^{\mathrm{DG}}}{L_{\mathrm{DG}}} i_d^{\mathrm{DG}} - \omega_{\mathrm{e}}^{\mathrm{DG}} i_q^{\mathrm{DG}} - \dfrac{\pi v_{\mathrm{b}}^{\mathrm{AC}} i_d^{\mathrm{DG}}}{3\sqrt{3} L_{\mathrm{DG}} \sqrt{(i_d^{\mathrm{DG}})^2 + (i_q^{\mathrm{DG}})^2}} u_{\mathrm{DG}} \\ \dot{\omega}_{\mathrm{e}}^{\mathrm{DG}} = \dfrac{M_{\mathrm{DG}}}{2J_{\mathrm{DG}}}\left(T_{\mathrm{t}}^{\mathrm{DG}} - \dfrac{3}{2}\dfrac{M_{\mathrm{DG}}}{2}\phi_{\mathrm{m}}^{\mathrm{DG}} i_q^{\mathrm{DG}}\right) \\ \dot{v}_{\mathrm{c}}^{\mathrm{AC}} = \dfrac{1}{C_{\mathrm{b}}^{\mathrm{AC}}}\left(\dfrac{\pi}{2\sqrt{3}}\sqrt{(i_d^{\mathrm{WG}})^2 + (i_q^{\mathrm{WG}})^2} u_{\mathrm{WG}} + \dfrac{\pi}{2\sqrt{3}}\sqrt{(i_d^{\mathrm{DG}})^2 + (i_q^{\mathrm{DG}})^2} u_{\mathrm{DG}} - i_L^{\mathrm{AC}}\right) \end{cases} \tag{11}$$

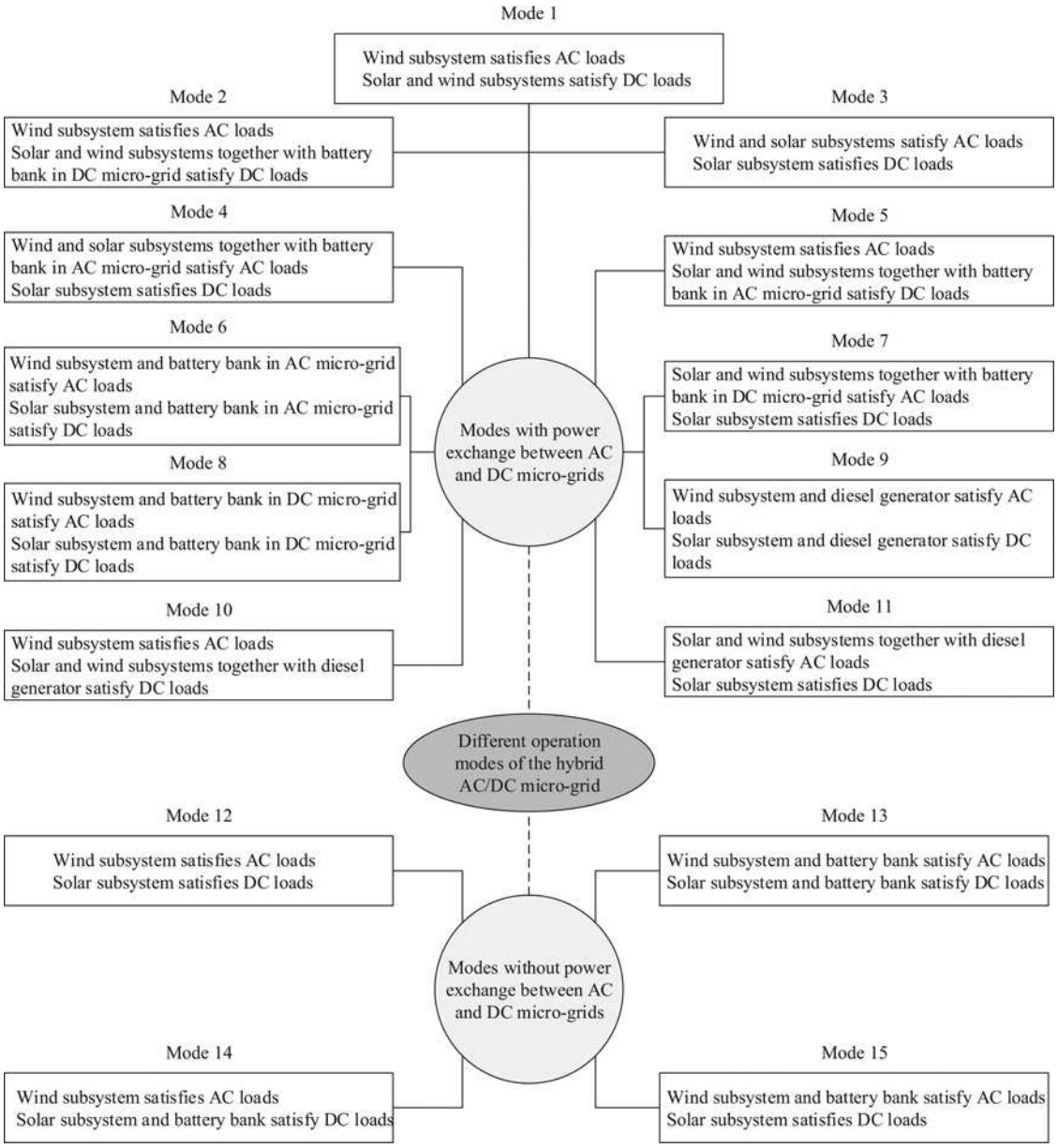

Fig. 2 *Different operating modes of the hybrid AC/DC micro-grid*

by solar subsystem to the DC load, as well as the battery bank. Also, the DC bus voltage (v_b^{DC}) is imposed by the battery bank connected to it. Assuming that the battery bank is modelled as a voltage source E_b^{DC} connected in series with a resistance R_b^{DC} and a capacitance C_b^{DC}, the dynamic model of the DC micro-grid may be written as [25]

$$\begin{cases} \dot{v}_{PV} = \dfrac{i_{PV}}{C} - \dfrac{i_o^{PV}}{C} u_{PV} \\ i_o^{PV} = -\dfrac{v_b^{DC}}{L} + \dfrac{v_{PV}}{L} u_{PV} \\ \dot{v}_c^{DC} = \dfrac{1}{C_b^{DC}} (i_o^{PV} - i_L^{DC}) \end{cases} \tag{14}$$

Thus, v_b^{DC} can also be calculated through the following equation

$$v_b^{DC} = E_b^{DC} + v_c^{DC} + (i_o^{PV} - i_L^{DC}) R_b^{DC} \tag{15}$$

The current i_m^{DC} shown in Fig. 1 corresponds to the power injected from the DC micro-grid to the AC micro-grid.

3 Supervisory controller design

In this paper, supervisory control for an isolated hybrid AC/DC micro-grid is considered. Operating modes of the micro-grid are divided into four different modes with no power exchange between the AC and DC micro-grids, and 11 modes with power exchange between the grids, as shown in Fig. 2. One of the main considerations here is to minimise utilisation of the DG with high priority, and restrict usage of the main converter with low priority. This will be explained in details as follows.

When the DC micro-grid injects power to the AC micro-grid, the AC power is obtained from two parallel connected DC/AC converters. Also, when the AC micro-grid injects power to the DC micro-grid, the main converter acts as an AC/DC converter. Thus, the DC power is obtained from two parallel-connected converters: (i) the DC/DC converter of the solar subsystem and (ii) the main converter. In both cases, it is shown that even small mismatches between the output voltages and impedances of the converters could degrade power quality [26, 27]. Nevertheless, forcing the micro-grids to work independently, may lead to not utilising maximum available wind or solar power and may hamper the efficiency of the system. Hence, a trade-off between the power

IET Renew. Power Gener., 2015, Vol. 9, Iss. 5, pp. 484–493

quality and the efficiency is considered as a basis for rule-based power management system. Thus, in our approach, when $\Delta P_{\mathrm{WG}} \geq P_{\mathrm{critical}}^{\mathrm{WG}}$, it indicates that unexploited wind power is high. Therefore power transfer from AC to DC micro-grid is permitted in order to utilise maximum available wind power. The same condition exists for the solar subsystem, such that $\Delta P_{\mathrm{PV}} \geq P_{\mathrm{critical}}^{\mathrm{Pv}}$ indicates the situation in which that the power transfer from DC to AC micro-grid is allowed, in order to utilise maximum available solar power. It is worth noting that, small values of the critical power prioritise utilising maximum available power, and consequently increase system efficiency. While, high values of the critical power prioritise achieving high power quality.

As shown in Fig. 2, operation mode 1 represents the conditions in which maximum available power is more than power demand, and the solar power is not sufficient to satisfy DC loads. Also, unexploited wind power is greater than the critical value, that is, $\Delta P_{\mathrm{WG}} \geq P_{\mathrm{critical}}^{\mathrm{WG}}$. In this mode, the main converter operates as an AC/DC rectifier, and injects the unexploited power of wind subsystem to the DC micro-grid. Mode 2 is similar to mode 1, unless maximum available power is less than power demand. Hence, wind and solar subsystems together with battery bank in the DC micro-grid satisfy DC loads. It should be remarked that when the battery bank in the DC micro-grid is fully discharged and maximum available power is more than power demand, the unexploited power of wind subsystem should be injected to the DC micro-grid regardless of the trade-off condition. Modes 3 and 4 are more or less similar to modes 1 and 2, respectively, however, in these modes the wind power is not sufficient to satisfy AC loads. Hence, in mode 3 the unexploited power of solar subsystem is injected to the AC micro-grid, and in mode 4, wind and solar subsystems together with battery bank in the AC micro-grid feed AC loads. It should be remarked that when the battery bank in the AC micro-grid is fully discharged and maximum available power is more than power demand, the unexploited power of solar subsystem should be injected to the AC micro-grid regardless of the trade-off condition. Now, let us assume a condition where battery bank in the DC micro-grid is discharged fully, the solar power is not sufficient to satisfy DC loads, and the wind subsystem is sufficient to satisfy AC loads. Also, maximum available power is less than power demand. In this mode, which is designated by mode 5, wind and solar subsystems together with battery bank in the AC micro-grid satisfies DC loads. Mode 6 is similar to mode 5, unless the wind subsystem is not sufficient to satisfy AC loads. Hence, battery bank in the AC micro-grid is utilised in order to satisfy a power shortage in both the AC and DC micro-grids, regardless on the trade-off condition. Modes 7 and 8 are similar to modes 5 and 6, respectively, unless the wind power is not sufficient to satisfy AC loads and the battery bank in the AC micro-grid is discharged fully. In mode 7, in which solar power is sufficient to satisfy DC loads, wind and solar subsystems together with battery bank in the DC micro-grid satisfy DC loads. Also, in mode 8, in which solar power is not sufficient to satisfy DC loads, battery bank in the DC micro-grid is utilised in order to satisfy a power shortage in both the AC and DC micro-grids, regardless on the trade-off condition. If maximum available power is less than power demand, and the battery banks are discharged fully, the DG is turned on. Mode 9 represents the condition in which solar and wind power are not sufficient to satisfy DC and AC loads, respectively. Hence, the DG is used to compensate power shortage in both AC and DC micro-grids, and the main converter operates as an AC/DC rectifier. In mode 10, wind subsystem is sufficient to cover AC loads. Thus, power shortage in DC micro-grid is supplied by the wind subsystem and the DG. In contrast with mode 10, in mode 11, solar subsystem is not sufficient to satisfy DC loads. Hence, wind and solar subsystems together with the DG are used to satisfy AC loads.

All the aforementioned operation modes correspond to conditions with power exchange between the AC and DC micro-grids. Now, let us argue the conditions in which there is no power exchange between the AC and DC micro-grids. Mode 12 represents sufficient wind and solar powers to satisfy the power demand by AC and DC micro-grids, respectively. Therefore, the wind and solar subsystems track the total AC and DC power demands, respectively, and both battery banks store energy following their recharge cycle. Mode 13 is characterised by both generation subsystems set to operate at their maximum energy conversion point, and the battery banks acting as power supplies instead as a recipient of energy. Hence, in mode 13, wind subsystem and battery bank in AC micro-grid satisfy AC loads, while DC loads are fed by solar subsystem together with battery bank in DC micro-grid. Mode 14 corresponds to the condition in which solar power is not sufficient to satisfy DC loads, and $\Delta P_{\mathrm{WG}} < P_{\mathrm{critical}}^{\mathrm{WG}}$. In this mode, and regardless of the amount of maximum available power, wind subsystem satisfies AC loads and solar subsystem together with battery bank in DC micro-grid satisfy DC loads. Mode 15 is similar to mode 14, unless wind power is not sufficient to satisfy AC loads, and $\Delta P_{\mathrm{PV}} < P_{\mathrm{critical}}^{\mathrm{PV}}$. Hence, solar subsystem satisfies DC loads, and wind subsystem together with battery bank in AC micro-grid satisfy AC loads.

According to the above definitions, the proposed supervisory controller is responsible to detect the operation mode of the hybrid AC/DC micro-grid and set the reference values of the wind and solar subsystems, as well as managing the recharge cycle of the battery banks. It is worth noting that the supervisor controller is designed such that the DG is in service only when the battery banks are discharged fully and cannot supply the power shortage.

As it is discussed above, the wind subsystem acts either satisfying power demand or tracking the wind turbine maximum power conversion. The operating mode of wind subsystem may be identified by using maximum available power $P_{\mathrm{max}}^{\mathrm{WG}}$. If $P_{\mathrm{max}}^{\mathrm{WG}} \geq qP_{\mathrm{ref}}^{\mathrm{WG}}$, the operating mode may be one of the modes 1, 2, 5 or 8. Otherwise, the operating mode would be one the modes 3, 4, 5, 6, 7 or 9. To control the wind subsystem, a sliding controller is used, which is in the following form

$$\begin{cases} \text{if } P_{\mathrm{max}}^{\mathrm{WG}} \geq P_{\mathrm{ref}}^{\mathrm{WG}} \Rightarrow u_{\mathrm{WG}} = u_{\mathrm{I}} \\ \text{if } P_{\mathrm{max}}^{\mathrm{WG}} < P_{\mathrm{ref}}^{\mathrm{WG}} \Rightarrow u_{\mathrm{WG}} = u_{\mathrm{II}} \end{cases} \tag{16}$$

where u_{I}, u_{II} can be calculated as given in [28], and the sliding surfaces are

$$\begin{aligned} h_1^{\mathrm{WG}} &= p_{\mathrm{ref}}^{\mathrm{WG}} - \frac{3}{2}\phi_{\mathrm{m}}^{\mathrm{WG}} i_q^{\mathrm{WG}} \omega_{\mathrm{e}}^{\mathrm{WG}} + \frac{3}{2}((i_q^{\mathrm{WG}})^2 + (i_d^{\mathrm{WG}})^2)R_{\mathrm{s}}^{\mathrm{WG}} \\ h_2^{\mathrm{WG}} &= P_{\mathrm{max}}^{\mathrm{WG}} - \frac{3}{2}\phi_{\mathrm{m}}^{\mathrm{WG}} i_q^{\mathrm{WG}} \omega_{\mathrm{e}}^{\mathrm{WG}} \end{aligned} \tag{17}$$

As mentioned above, the DG will be in service to supply the power shortage in both micro-grids. Consequently, with sufficient wind and solar power the DG is off. In this paper, the control objective corresponding to DG is to enforce the DG to operate at the maximum power generation point. For this purpose and similar to WG, a sliding mode control is presented which the sliding surface is as follows

$$h_{\mathrm{DG}} = p_{\mathrm{max}}^{\mathrm{DG}} - \frac{3}{2}\phi_{\mathrm{m}}^{\mathrm{DG}} i_q^{\mathrm{DG}} \omega_{\mathrm{e}}^{\mathrm{DG}} \tag{18}$$

where $p_{\mathrm{max}}^{\mathrm{DG}}$ is the maximum power of the DG. Using a general sliding mode control design method based on a differential geometric approach, the control results

$$u_{\mathrm{DG}} = \left[-\frac{f_1}{g_1} - \frac{i_q^{\mathrm{DG}} f_2}{\omega_{\mathrm{e}}^{\mathrm{DG}} g_1} \right] + \left(\sigma |h_{\mathrm{DG}}| + \xi_{\mathrm{max}} \left\| \frac{\partial h_{\mathrm{DG}}}{\partial x} \right\|_2 \right) \frac{2\mathrm{sign}(h_{\mathrm{DG}})}{3\phi_{\mathrm{m}}^{\mathrm{DG}} \omega_{\mathrm{e}}^{\mathrm{DG}} g_1} \tag{19}$$

where σ and $\xi_{\max}$ are design constants, and

$$\left\|\frac{\partial h_{\mathrm{DG}}}{\partial x}\right\|_2 = \sqrt{\left(\frac{3}{2}\phi_{\mathrm{m}}^{\mathrm{DG}}\omega_{\mathrm{e}}^{\mathrm{DG}}\right)^2 + \left(\frac{3}{2}\phi_{\mathrm{m}}^{\mathrm{DG}} i_q^{\mathrm{DG}}\right)^2}$$

$$f_1 = -\frac{R_{\mathrm{s}}^{\mathrm{DG}}}{L_{\mathrm{DG}}} i_q^{\mathrm{DG}} - \omega_{\mathrm{e}}^{\mathrm{DG}} i_d^{\mathrm{DG}} + \frac{\omega_{\mathrm{e}}^{\mathrm{DG}}\phi_{\mathrm{m}}^{\mathrm{DG}}}{L_{DG}}$$

$$f_2 = \frac{M_{\mathrm{DG}}}{2J_{\mathrm{DG}}}\left(T_{\mathrm{t}}^{\mathrm{DG}} - \frac{3}{2}\frac{M_{\mathrm{DG}}}{2}\phi_{\mathrm{m}}^{\mathrm{DG}} i_q^{\mathrm{DG}}\right)$$

$$g_1 = -\frac{\pi v_{\mathrm{b}}^{\mathrm{AC}} i_q^{\mathrm{DG}}}{3\sqrt{3}L_{\mathrm{DG}}\sqrt{(i_d^{\mathrm{DG}})^2 + (i_q^{\mathrm{DG}})^2}} u_{\mathrm{DG}}$$

$$x = [i_q^{\mathrm{DG}}\ i_d^{\mathrm{DG}}\ \omega_{\mathrm{e}}^{\mathrm{DG}}]^{\mathrm{T}}$$

It should be remarked that for minimising the fuel consumption by the DG, a PI controller is used to regulate the maximum power of the DG to the power demand reference $p_{\mathrm{ref}}^{\mathrm{DG}}$.

The solar subsystem also acts either satisfying power demand or tracking the PV array maximum power conversion. It is important to remark that the solar cell voltage corresponding to maximum PV array power ($v_{\mathrm{max}}^{\mathrm{PV}}$) may be calculated through the follows algebraic equation

$$\frac{\partial P_{\mathrm{PV}}}{\partial v_{\mathrm{PV}}} = 0 \rightarrow \left(\frac{q v_{\mathrm{max}}^{\mathrm{PV}}}{n_{\mathrm{s}} AKT} + 1\right) e^{q v_{\mathrm{max}}^{\mathrm{PV}}/n_{\mathrm{s}}\mathrm{AKT}} = \frac{I_{\mathrm{ph}} + I_{\mathrm{rs}}}{I_{\mathrm{rs}}} \tag{20}$$

and the current corresponding to maximum PV array power ($i_{\mathrm{max}}^{\mathrm{PV}}$) can be obtained by (12) substituting $v_{\mathrm{max}}^{\mathrm{PV}}$. Thus, for $p_{\mathrm{max}}^{\mathrm{PV}} \geq p_{\mathrm{ref}}^{\mathrm{PV}}$, the operating mode of the hybrid AC/DC micro-grid would be one of the modes 1, 3, 6 or 9, according to other components condition. However, if $p_{\mathrm{max}}^{\mathrm{PV}} < p_{\mathrm{ref}}^{\mathrm{PV}}$, the operating mode would be one of the modes 2, 4, 5, 7 or 8. In order to enforce the solar subsystem to track the reference power, a sliding controller is used in this paper. The control law can be expressed in the following form

$$\begin{cases} \text{if } P_{\mathrm{max}}^{\mathrm{PV}} \geq P_{\mathrm{ref}}^{\mathrm{PV}} \Rightarrow u_{\mathrm{PV}} = \begin{cases} 1, & \text{if } h_1^{\mathrm{PV}} \geq 0 \\ 0, & \text{if } h_1^{\mathrm{PV}} < 0 \end{cases} \\ \text{if } P_{\mathrm{max}}^{\mathrm{PV}} < P_{\mathrm{ref}}^{\mathrm{PV}} \Rightarrow u_{\mathrm{PV}} = \begin{cases} 1, & \text{if } h_2^{\mathrm{PV}} \geq 0 \\ 0, & \text{if } h_2^{\mathrm{PV}} < 0 \end{cases} \end{cases} \tag{21}$$

where the sliding surfaces are as follows

$$\begin{aligned} h_1^{\mathrm{PV}} &= P_{\mathrm{ref}}^{\mathrm{PV}} - i_{\mathrm{o}}^{\mathrm{PV}} v_{\mathrm{b}}^{\mathrm{DC}} = 0 \\ h_2^{\mathrm{PV}} &= P_{\mathrm{max}}^{\mathrm{PV}} - i_{\mathrm{o}}^{\mathrm{PV}} v_{\mathrm{b}}^{\mathrm{DC}} = 0 \end{aligned} \tag{22}$$

Since the proposed hybrid micro-grid is a non-linear system (converters are not ideal in reality) and fuzzy logic can offer a practical way for designing nonlinear control systems, a fuzzy controller is considered to maintain battery banks SOC. SOC of battery banks can be calculated by $\mathrm{SOC_k} = (\int_0^t i_{\mathrm{b}}^{\mathrm{k}}(\tau)\mathrm{d}\tau)/(Q_{\mathrm{c},k}^{\max})$. To obtain the desired SOC value, the fuzzy controller is designed to be in charging mode or discharging mode for the proposed hybrid AC/DC micro-grid, [29, 30]. The input variables of the fuzzy controller are $\Delta\mathrm{SOC}_k$ and ΔP_k and output variable is i_{b}^k, where $\Delta\mathrm{SOC}_k = \mathrm{SOC}_k - \mathrm{SOC}_k^{\mathrm{des}}$, and $\Delta P_k = P_{\mathrm{gen}}^k - P_L^k$, $k = \{\mathrm{AC}, \mathrm{DC}\}$. Also, $\mathrm{SOC}_k^{\mathrm{des}} = 1$ is assumed in this paper. The input and the output membership functions of fuzzy control contain five grades: NB (negative big), NS (negative small), ZO (zero), PS (positive small) and PB (positive big), as shown in Fig. 3. It should be remarked that the membership functions are defined by trial and error. The control rules of the fuzzy controller prioritise maintaining the desired SOC of battery banks. For example, the output variable i_{b}^k is PB (the degree of charging current is PB) when the input variable ΔP_k is PB and $\Delta\mathrm{SOC}_k$ is either NB or NS, that is, charging the battery banks to desired SOC figure high in fuzzy controller responsibilities.

The proposed supervisory controller can be formalised using a state machine approach, which is a powerful tool to implement decision making algorithms [10]. The state-chart representing the proposed supervisory controller is given in Fig. 4, where

$$S = \{s_1, s_2, s_3, s_4, s_5, s_6, s_7, s_8, s_9, s_{10}, s_{11}, s_{12}, s_{13}, s_{141}, s_{142}, s_{151}, s_{152}\}$$

is the set of all nodes in the state-chart, $\Sigma = \{1, \ldots, 12\}$ is the set of possible input events given in Fig. 4. It is worth noting that $s_1, \ldots, s_{13}$ correspond to operating modes 1, …, 13, respectively. Operating mode 14 is further classified as s_{141} and s_{142}, where in s_{141} maximum available power is more than demanded power, and in s_{142} maximum available power is less than demanded power. Operating mode 15 is also classified as s_{151} and s_{151}, where in s_{151} maximum available power is more than demanded power and in s_{151} maximum available power is less than demanded power.

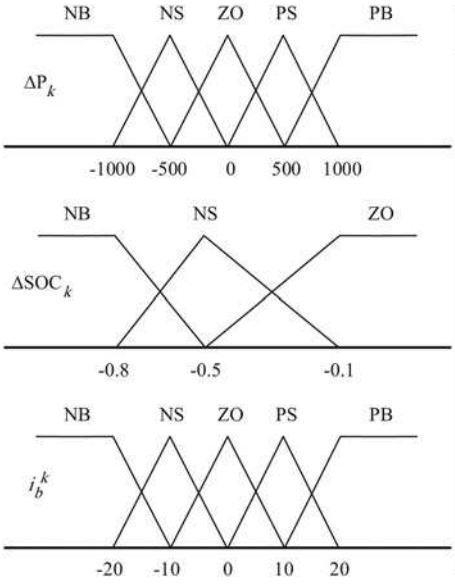

No.	Rule
1	if ΔP is PB and ΔSOC is NB, then i_b is PB
2	if ΔP is PB and ΔSOC is NS, then i_b is PB
3	if ΔP is PB and ΔSOC is ZO, then i_b is ZO
4	if ΔP is PS and ΔSOC is NB, then i_b is PS
5	if ΔP is PS and ΔSOC is NS, then i_b is PS
6	if ΔP is PS and ΔSOC is ZO, then i_b is ZO
7	if ΔP is ZO and ΔSOC is NB, then i_b is ZO
8	if ΔP is ZO and ΔSOC is NS, then i_b is ZO
9	if ΔP is ZO and ΔSOC is ZO, then i_b is ZO
10	if ΔP is NS and ΔSOC is NB, then i_b is ZO
11	if ΔP is NS and ΔSOC is NS, then i_b is NS
12	if ΔP is NS and ΔSOC is ZO, then i_b is NS
13	if ΔP is NB and ΔSOC is NB, then i_b is ZO
14	if ΔP is NB and ΔSOC is NS, then i_b is NB
15	if ΔP is NB and ΔSOC is ZO, then i_b is NB

Fig. 3 *Input and output membership functions, and the control rules of fuzzy controller*

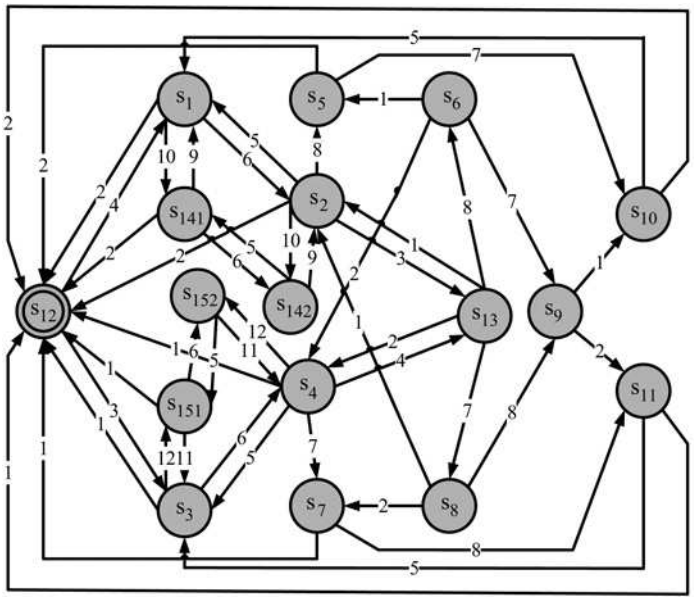

Event	Decription
1	$P_{max}^{WG} \geq P_L^{AC}$
2	$P_{max}^{PV} \geq P_L^{DC}$
3	$P_{max}^{WG} < P_L^{AC}$
4	$P_{max}^{PV} < P_L^{DC}$
5	$P_{max}^{WG} + P_{max}^{PV} \geq P_L^{AC} + P_L^{DC}$
6	$P_{max}^{WG} + P_{max}^{PV} < P_L^{AC} + P_L^{DC}$
7	$SOC_{AC} < 0.2$
8	$SOC_{DC} < 0.2$
9	$\Delta P_{WG} \geq P_{critical}^{WG}$
10	$\Delta P_{WG} < P_{critical}^{WG}$
11	$\Delta P_{PV} \geq P_{critical}^{PV}$
12	$\Delta P_{PV} < P_{critical}^{PV}$

Fig. 4 *Schematic diagram of the supervisory controller based on state machine approach*

Table 1 Parameters used in simulations

Parameter	Value	Parameter	Value
ρ	1.225 kg/m^3	A	10.6362 m^2
r	1.84 m	R_s^{WG}, R_s^{DG}	0.3676 Ω
L_{WG}, L_{DG}	3.55 mH	ϕ_m^{WG}, ϕ_m^{DG}	0.2876 Wb
M_{WG}, M_{DG}	28	E_b^{AC}, E_b^{DC}	50 V
R_b^{AC}, R_b^{DC}	14 mΩ	C_b^{AC}, C_b^{DC}	180 000 F
λ_{opt}	8.1	I_{scr}	3.27 A
K_i	0.0017 A°C	J_{WG}, J_{DG}	7.856 kg m^2
I_{rr}	2.079×10^{-6} A	T_r	301.18 K
E_G	1.1 V	K	1.380×10^{-23} Nm/K
n_p, n_s	5 and 200	$P_{critical}^{WG}$, $P_{critical}^{PV}$	200 W
q	1.6×10^{-19} C	B	1.6
$Q_{c,AC}^{max}$, $Q_{c,DC}^{max}$	80 A h	k_{pm}	1
τ_{pm}	0.2	t_d	0.011 s
σ	5	ξ_{max}	0.02

4 Simulation results

In this section, a sample hybrid AC/DC micro-grid is simulated to assess the performance of the proposed supervisory controller, and to demonstrate its effectiveness. In the following simulations, the main converter is assumed to be ideal, that is, in modes 1, 2, 5, 6, 9 and 10 it acts as an ideal rectifier, and in modes 3, 4, 7, 8 and 11 it acts as an ideal static inverter. The parameters used in the simulation are also given in Table 1. It should be remarked that the steps in the load current profile refer to abrupt load connection or disconnection. Furthermore, positive and negative values of battery banks power correspond to the charge and discharge conditions, respectively.

Simulation results, presented in Figs. 5–8, indicate that the system starts from mode 12, where both micro-grids satisfy their power demand by using wind and solar subsystems. For $t \in [4, 5.45]$(s), the operating mode is 13, and the battery banks supply the power shortage in the both AC and DC micro-grids. For $t \in [5.45, 6.45]1$ (s), the battery bank in AC micro-grid has been fully discharged, and the battery bank in DC micro-grid supply the power shortage in the both AC and DC micro-grids. After $t = 6.451$(s), the DG turns on to supply the power shortage in both micro-grids. For $t \in [6.45, 8.30]1$(s), $t \in [8.77, 9.00]1$(s), $t \in [9.71, 10.70]1$(s) and $t \in [11.55, 15.85]1$(s), the operating mode is 9, in which the DG supply power shortage in the both AC and DC micro-grids. For $t \in [8.30, 8.77]1$(s), $t \in [9.00, 9.71]1$(s) and $t \in [10.70, 11.55]1$(s), the DG and the wind subsystem supply the power shortage in the DC micro-grid. Thus, the operation mode is 10. For $t \in [15.85, 17.83]1$(s), the DG and the solar subsystem supply the power shortage in the AC micro-grid. After $t = 17.831$(s), the solar power is sufficient to satisfy power demanded by DC loads, and maximum available power is more than power demand. Thus, for $t \in [17.83, 18.48]1$(s), the operation mode is 3, and solar and wind subsystem satisfies the power demand in the AC micro-grid. For $t \in [18.48, 22.00]$, the operation mode is 11, and the diesel generation is in service again to satisfy power demanded in the

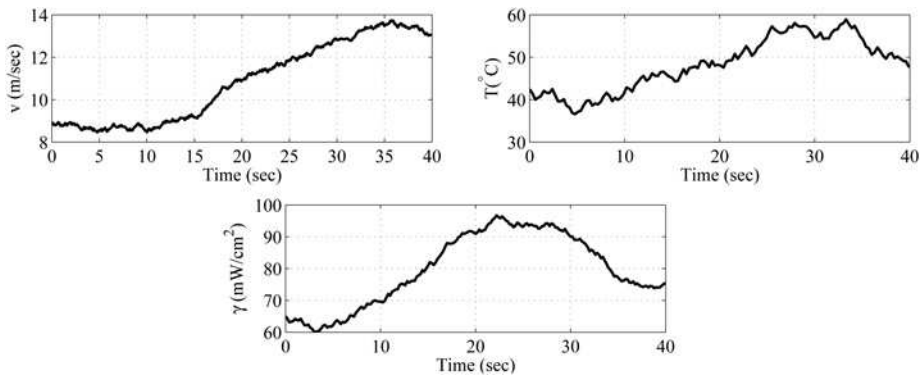

Fig. 5 *Weather condition: wind speed (v), cell temperature (T) and solar radiation (γ)*

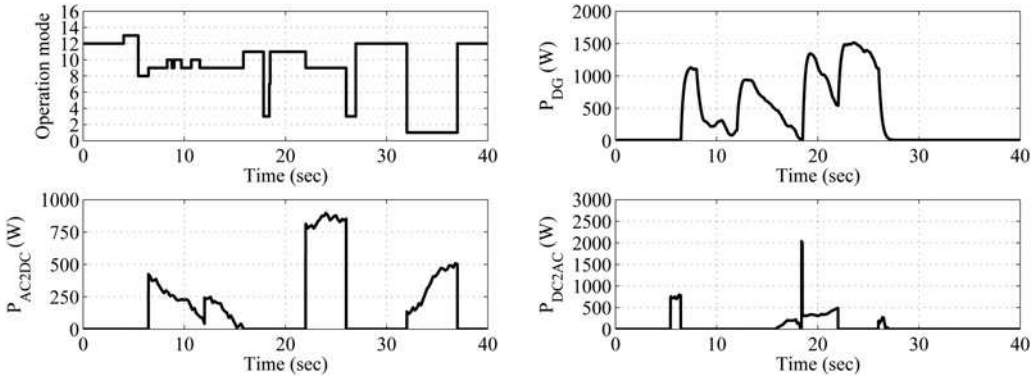

Fig. 6 *Determined operation modes of the hybrid AC/DC micro-grid, the power generated by the DG (P_{DG}), power injected from the DC micro-grid to the AC micro-grid (P_{DC2AC}) and power injected from the AC micro-gridto the DC micro-grid (P_{AC2DC})*

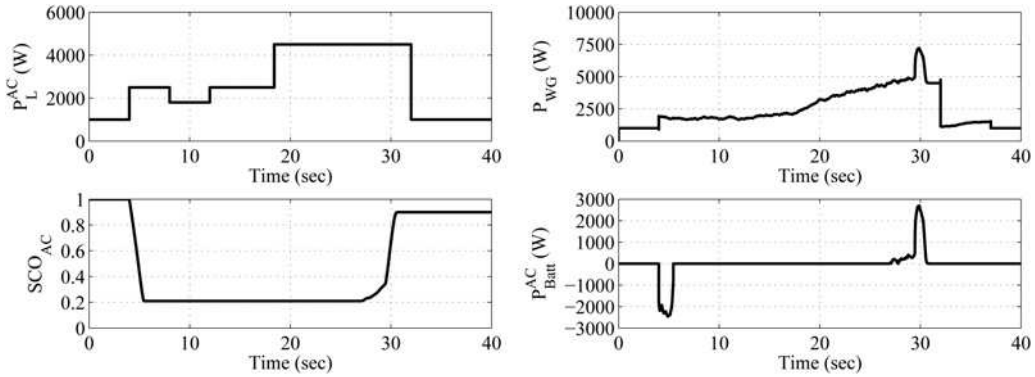

Fig. 7 *Dynamic response of the AC micro-grid; load current (P_L^{AC}), power generated by the wind subsystem (P_{WG}), SOC of the battery bank (SOC_{AC}) and power profile of the battery bank (P_{Batt}^{AC})*

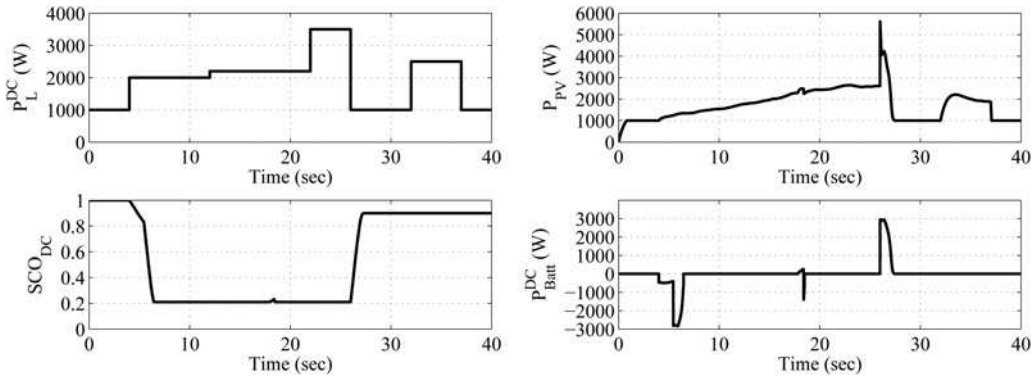

Fig. 8 *Dynamic response of the DC micro-grid; load current (P_L^{DC}), power generated by the solar subsystem (P_{PV}), SOC of the battery bank (SOC_{DC}) and power profile of the battery bank (P_{Batt}^{DC})*

AC micro-grid. Also, for $t \in [22.00, 26.00]1$(s), the DG supply power shortage in the both AC and DC micro-grids. For $t \in [26.00, 26.95]1$(s), the solar power is sufficient to satisfy power demanded by DC loads, and maximum available power is more than power demand. Hence, the operation mode is 3, and the solar subsystem supply power shortage in the AC micro-grid. After $t = 26.951$(s), wind and solar powers are sufficient to satisfy power demand in AC and DC micro-grids, respectively. This condition, which corresponds to mode 12, lasts until $t = 321$(s). For $t \in [32.00, 37.00]1$(s), maximum available power is more than power demand, and also $\Delta P_{PV} \geq P_{critical}^{PV}$. Hence, the operation mode is 1, and the solar subsystem supply power shortage in the AC micro-grid. Finally, the mode returns to 12 and the wind subsystem and the solar subsystem provide the corresponding power demand.

5 Conclusion

In this paper, a supervisory controller based on the state machine approach for an isolated hybrid AC/DC micro-grid is proposed to satisfy load power demand in both the AC and DC micro-grids, while maintaining SOC of battery banks with fuzzy control. First step in designing the supervisor controller was distinguishing

different operation modes of the system. Here, 15 distinct operation modes were considered, where 4 modes correspond to situations without power exchange between the AC and DC micro-grids, and 11 modes indicate situations with power exchange between the AC and DC micro-grids. Also, the DG will be in service when wind and solar subsystems cannot satisfy the power demand. Using the state machine approach, reference values of generation subsystems were set by supervisory controller following a pre-defined strategy. Based on the difference of generated and demanded power, as well as SOC, charge and discharge cycles of battery banks are determined using a fuzzy controller. The resulting performance was evaluated through the study of an example. Simulation results verified the effectiveness of the proposed supervisor controller.

6 References

1 Gupta, A., Saini, R.P., Sharma, M.P.: 'Steady-state modelling of hybrid energy system for off grid electrification of cluster of villages', *Renew. Energy*, 2010, **35**, (2), pp. 520–535
2 Eghtedarpour, N., Farjah, E.: 'Distributed charge/discharge control of energy storages in a renewable-energy-based DC micro-grid', *IET Renew. Power Gener.*, 2014, **8**, (1), pp. 45–57
3 Piagi, P., Lasseter, R.H.: 'Autonomous control of microgrids'. Proc. IEEE Pow. Eng. Soc. General Meeting, Montreal, Quebec, Canada, June 2006, pp. 496–503
4 Chiang, H.C., Ma, T.T., Cheng, Y.H., Chang, J.M., Chang, W.N.: 'Design and implementation of a hybrid regenerative power system combining grid tie and uninterruptible power supply functions', *IET Renew. Power Gener.*, 2010, **4**, (1), pp. 85–99
5 Morias, H., Kadar, P., Faria, P., Vale, Z.A., Khodr, H.M.: 'Optimal scheduling of a renewable micro-grid in an isolated load area using mixed-integer linear programming', *Renew. Energy*, 2010, **35**, (1), pp. 151–156
6 Pipattanasomporn, M., Feroze, H., Rahman, S.: 'Securing critical loads in a PV-based microgrid with a multi-agent system', *Renew. Energy*, 2012, **39**, (1), pp. 166–174
7 Sechilariu, M., Wang, B.C., Locment, F.: 'Supervision control for optimal energy cost management in DC microgrid: Design and simulation', *Int. J. Electr. Power*, 2014, **58**, pp. 140–149
8 Chen, C., Duan, S., Cai, T., Liu, B., Hu, G.: 'Smart energy management system for optimal microgrid economic operation', *IET Renew. Power Gener.*, 2011, **5**, (3), pp. 258–267
9 Valenciaga, F., Puleston, P.F.: 'Supervisory control for a stand-alone hybrid generation system using wind and photovotaic energy', *IEEE Trans. Energy Convers.*, 2005, **20**, (2), pp. 398–405
10 Feroldi, D., Degliuomini, L.N., Basualdo, M.: 'Energy management of a hybrid system based on wind-solar power sources and bioethanol', *Chem. Eng. Res. Des.*, 2013, **91**, (8), pp. 1440–1455
11 Kanchev, H., Lu, D., Colas, F., Lazarov, V., Francois, B.: 'Energy management and operational planning of a microgrid with a PV-based active generator for smart grid applications', *IEEE Trans. Ind. Electron.*, 2011, **58**, (10), pp. 4583–4592
12 Teleke, S., Baran, M.E., Bhattacharya, S., Huang, A.Q.: 'Rule-based control of battery energy storage for dispatching intermittent renewable sources', *IEEE Trans. Sustain. Energy*, 2010, **1**, (3), pp. 117–124
13 Wang, C., Nehrir, M.H.: 'Power management of a stand-alone wind/photovoltaic/fuel cell energy system', *IEEE Trans. Energy Convers.*, 2008, **23**, (3), pp. 957–967
14 Hajizadeh, A., Golkar, M.A.: 'Intelligent power management strategy of hybrid distributed generation system', *Int. J. Electr. Power*, 2007, **29**, (10), pp. 783–795
15 Jiang, Z., Gao, L., Dougal, R.A.: 'Adaptive control strategy for active power sharing in hybrid fuel cell/battery power sources', *IEEE Trans. Energy Convers.*, 2007, **22**, (2), pp. 507–515
16 Jeong, K.S., Lee, W.Y., Kim, C.S.: 'Energy management strategies of a fuel cell/battery hybrid system using fuzzy logics', *J. Power Sources*, 2005, **145**, (2), pp. 319–326
17 Wang, P., Geol, L., Liu, X., Choo, F.H.: 'Harmonizing AC and DC: A hybrid AC/DC future grid solution', *IEEE Power Energy Mag.*, 2013, **11**, (3), pp. 76–83
18 Liu, X., Wang, P., Loh, P.C.: 'A hybrid AC/DC micro-grid'. Proc. Int. Power Electron. Conf., Singapore, October 2010, pp. 746–751
19 Liu, X., Wang, P., Loh, P.C.: 'A hybrid AC/DC microgrid and its coordination control', *IEEE Trans. Smart Grid*, 2011, **2**, (2), pp. 278–286
20 Kamel, R.M., Chaouachi, A., Nagasaka, K.: 'Wind power smoothing using fuzzy logic pitch controller and energy capacitor system for improvement micro-grid performance in islanding mode', *Energy*, 2010, **35**, (5), pp. 2119–2129
21 Valenciaga, F., Puleston, P.F., Battaiotto, P.E., Mantz, R.J.: 'Passivity/sliding mode control of a stand-alone hybrid generation system', *IEE Proc., Control Theory Appl.*, 2000, **147**, (6), pp. 680–686
22 Torres, M., Lopes, L.A.C.: 'Virtual synchronous generator control in autonomous wind-diesel power systems'. Proc. IEEE Elect. Power Energy Conf., Montreal, Quebec, Canada, October 2009, pp. 1–6
23 Jenkins, D.P., Fletcher, J., Kane, D.: 'Lifetime prediction and sizing of lead-acid batteries for microgeneration storage applications', *IET Renew. Power Gener.*, 2008, **2**, (3), pp. 191–200
24 Hussein, K.H., Muta, I., Hoshino, T., Osakada, M.: 'Maximum photovoltaic power tracking: an algorithm for rapidly changing atmospheric conditions', *IEE Proc., Gener. Transm. D*, 1995, **142**, (1), pp. 59–64
25 Valenciaga, F., Puleston, P.F., Battaiotto, P.E.: 'Power control of a photovoltaic array in a hybrid electric generationn system using sliding mode techniques', *IEE Proc., Control Theory Appl.*, 2001, **148**, (6), pp. 448–455
26 Prodanovic, M., Green, T.C.: 'High-quality power generation through distributed control of a power park microgrid', *IEEE Trans. Ind. Electron.*, 2006, **53**, (5), pp. 1471–1482
27 Guerrero, J.M., Vasquez, J.C., Matas, J., Vicuna, L.G.D., Castilla, M.: 'Hierarchical control of droop-controlled AC and DC microgrids-a general approach toward standardization', *IEEE Trans. Ind. Electron.*, 2011, **58**, (1), pp. 158–172
28 Valenciaga, F., Puleston, P.F., Battaiotto, P.E.: 'Variable structure system control design method based on a differential geometric approach: application to a wind energy conversion subsystem', *IEE Proc., Control Theory Appl.*, 2004, **151**, (1), pp. 6–12
29 Chen, Y.K., Wu, Y.C., Song, C.C., Chen, Y.S.: 'Design and implementation of energy management system with fuzzy control for DC micro-grid systems', *IEEE Trans. Power Electron.*, 2013, **28**, (4), pp. 1563–1570
30 Hajizadeh, A., Golkar, M.A.A.: 'Fuzzy neural control of a hybrid fuel cell/battery distributed power generation system', *IET Renew. Power Gener.*, 2009, **3**, (4), pp. 402–414